

Amyloid-like protein formation and aortic valve calcification promoted by oxidative stress

I. Mamarelis^{1*}, E. Koutoulakis², Ch. Kotoulas³, V. Dritsa⁴, V. Mamareli⁴, K. Pissaridi³, M. Kyriakidou⁴, J. Anastassopoulou^{4,5}

¹Department of Cardiology, NIMTS Veterans Army Hospital of Athens, Greece

²Department of Cardiology, 401 Army General Hospital of Athens, Greece

³Cardiac Surgery Department, 401 Army General Hospital of Athens, Greece

⁴National Technical University of Athens, Chemical Engineering Department, Radiation Chemistry & Biospectroscopy, Zografou Campus, 15780, Athens, Greece

⁵International Anticancer Research Institute, 1st km Kapandritiou-Kalamou Road, P.O. Box 22, Kapandriti, Attiki, 19014, Greece

Abstract

The mechanism of amyloid-like protein formation on aortic valve calcification and stenosis during oxidative stress was evaluated by using Attenuated total reflection Fourier transform infrared spectroscopy scanning electron microscopy and X-Ray diffraction. The high intensity bands of infrared spectra arising from the vibration modes of νCH_3 and νCH_2 of membranes' lipids are related with increasing of lipophilic environment due to amyloid-like protein formation. The shifts to lower frequencies of Amide I/Amide II absorptions are associated with the transformation of α -helix to β -parallel and β -antiparallel sheets confirming the amyloid development. The formation of hydroxyapatite and CaHPO_4 was supported by XRD analysis. The data showed that oxidative stress is a pathway of amyloid-like protein formation and the disulfide (S-S) bonds are the sites of calcium deposition.

Key words: aortic valve stenosis; aortic valve calcification; amyloid proteins; fourier transform infrared spectroscopy; scanning electron microscopy; X-Ray diffraction

SUBMISSION: 16/04/2016 | ACCEPTANCE: 07/06/2016

Citation

Mamarelis I, Koutoulakis E, Kotoulas Ch, et al. Amyloid like protein formation and aortic valve calcification promoted by oxidative stress. *Hell J Atheroscler* 2016, 7: 84-96

*Corresponding author: Jane Anastassopoulou, National Technical University of Athens, Chemical Engineering Department, Radiation Chemistry & Biospectroscopy, Zografou Campus, 15780, Athens, Greece. Tel: (+30) 6973013308, E-mail: ianastas@central.ntua.gr

Table 1. Patients' characteristic risk factors

Sex	Female	%	Male	%
Diabetes	4	31	23	56
Hyperlipidemia	7	54	18	44
Hypertension	9	69	28	68
Hyperuricemia	4	31	19	46
Smoking	5	38	35	85
Positive family history	8	61	27	66

1. Introduction

Calcified aortic valve stenosis remains the most common abnormality leading to heart valve replacement.^{1,2} It is estimated that in approximately 2% of elderly population (over 65 years) aortic valve sclerosis is present.³ Otto et al. suggested that the disease is not only age related but depends on other factors too, since they found that 40% of the patients with valve sclerosis have significant coronary artery disease without stenosis.⁴ There is a growing body of scientific papers of clinical and animal models suggesting that the pathogenesis of aortic valve stenosis is a multifunctional process and is associated with age, hypertension, hypercholesterolemia, diabetes, chronic inflammation and other risk factors and diets^{5,6} but the mechanism of the valve calcification remains still unclear. In modern clinical application the quantitative analytical tests play a pivotal role for monitoring and detection of the development of the disease, but the existing analytical methods do not give any answer about the conformational changes at the molecular level. Infrared spectroscopy is a sensitive nondestructive technique for analysis in order to detect the differences between "diseased" and "healthy" tissues or fluids from the characteristic spectral bands.⁷⁻¹⁴ The method is based on the interaction between infrared rays and the tissues (aortic valve, carotid or coronary artery, etc.) which give rise to the vibration of the characteristic chemical groups of biomolecules, such as NH, COO⁻, PO₄²⁻, PO₄³⁻, e.g.

of proteins, amino acids, DNA or hydroxyapatite, respectively.¹⁴⁻¹⁶ Each band is characteristic and appears at the same characteristic wavenumbers (cm⁻¹). The exact position of the bands depends on electron-withdrawing or donating effects of the intra- and inter-molecular environment in which the molecules are vibrating. This sensitivity of IR spectroscopy gives us the ability to gain information, at a molecular level, which is associated with certain diseases.⁷⁻¹⁶ The advantage of infrared spectroscopy is that allows a straightforward multicomponent analysis by recording their spectrum and it requires only few μm of *ex vivo* tissue sample or μg of biofluids, without any special preparation, such as demineralization or coloring with chromatin as is done in histological evaluation.

2. Patients

Fifty four representative specimens of human aortic valves were examined *ex vivo*. The patients, 13 women and 41 men aged 38-83 years old, presented with severe aortic stenosis and underwent aortic valve replacement under cardiopulmonary bypass. The risk factors of patients according to their biochemical measurements and clinical history are given in **Table 1**. In the group of women (**Table 1**) showed: Diabetes four (31%), hyperlipidemia seven (54%), hypertension nine (69%), hyperuricemia four (31%), smoking five (38%) and eight (61%) with positive family history of coronary artery disease. One woman was found with mitral valve stenosis had a history

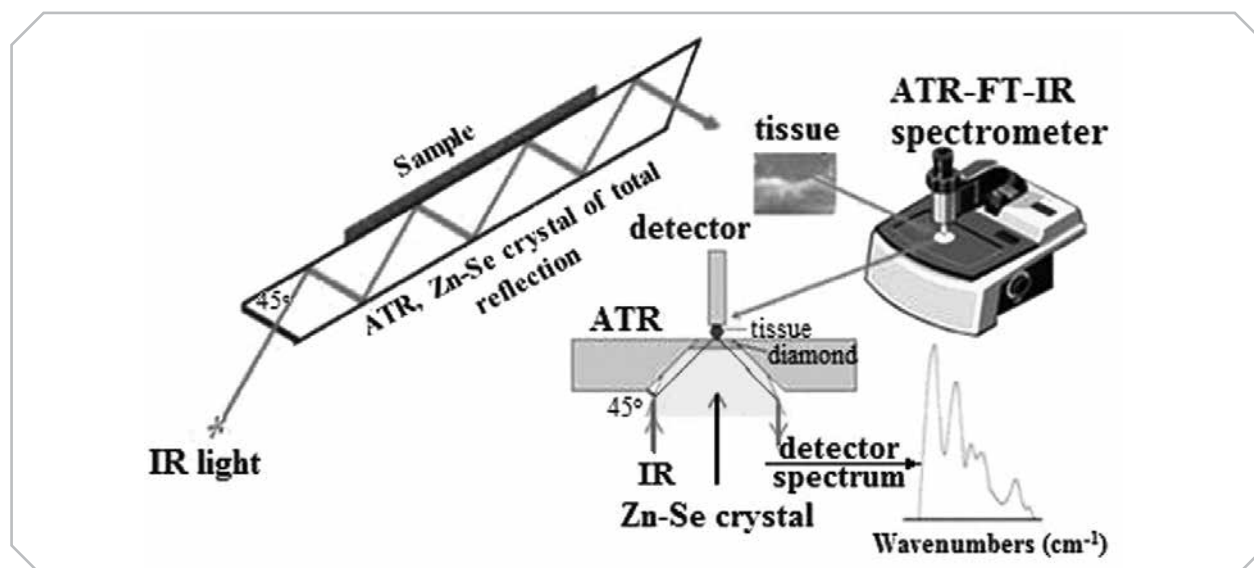


Figure 1. Schematic presentation of attenuated total reflection-Fourier transform infrared technique (ATR-FT-IR). The Infrared light passes through a Zn-Se crystal and after multiplication the beam is collected by a detector

of rheumatic fever in childhood. In the group of men (**Table 1**) twenty three were diabetic (56%), eighteen with hyperlipidemia (44%), twenty-eight with hypertension (68%), nineteen with hyperuricaemia (46%), and thirty-five smokers (85%) and twenty-five with positive family history of coronary disease (66%). A patient with coronary disease also had atrial septal defect and a history of sleep apnea, but not obese. Two patients had two-fold aortic valve (congenital anomaly), which showed stenosis and underwent valve replacement and one of them had coronary disease. Three patients reported occupational exposure to heavy metals (photographer, metallurgist, dental technician). Comparison between the two groups showed that men reflected almost all the risk factors, while the women showed to be more hyperlipidemic and hypertensive.

The samples were taken after the surgery of the patients according to the Greek ethical rules and the permission of the Scientific board of the 401 Army General and the National Technical University of Athens.

2.1. ATR-FT-IR spectrometer

The specimens were fixed in buffered formaldehyde solution immediately after the removal. The FT-

IR spectra were recorded with a Nicolet 6700 thermoscientific spectrometer, equipped with an Attenuated Total Reflection (ATR) accessory (**Figure 1**). Each spectrum consisted of 120 co-added spectra at a spectral resolution of 4 cm^{-1} and the OMNIC 7.2a software was used for data analysis.

The IR light passes through a Zn-Se crystal and after multiplication of the internal reflections on the sample the beam is collected by a detector and is transformed to spectrum. The diamond increases the ratio of signal to noise and thus minimizes the size of the sample. Modern infrared spectrometers are equipped with Attenuated total reflection apparatus and diamond crystal, which allow the detection of smaller sample amount and they do not need any special preparation.

2.2. Scanning Electron Microscope (SEM)

Scanning electron microscope from Fei Co, The Netherlands, was used for the detection of aortic valve surface architecture. SEM was combined with Energy Dispersive X-Ray (EDX) apparatus for the chemical elemental composition analysis in different sites of the aortic valves and tissues. It must be noticed that there was not any coating of the samples with carbon or gold.

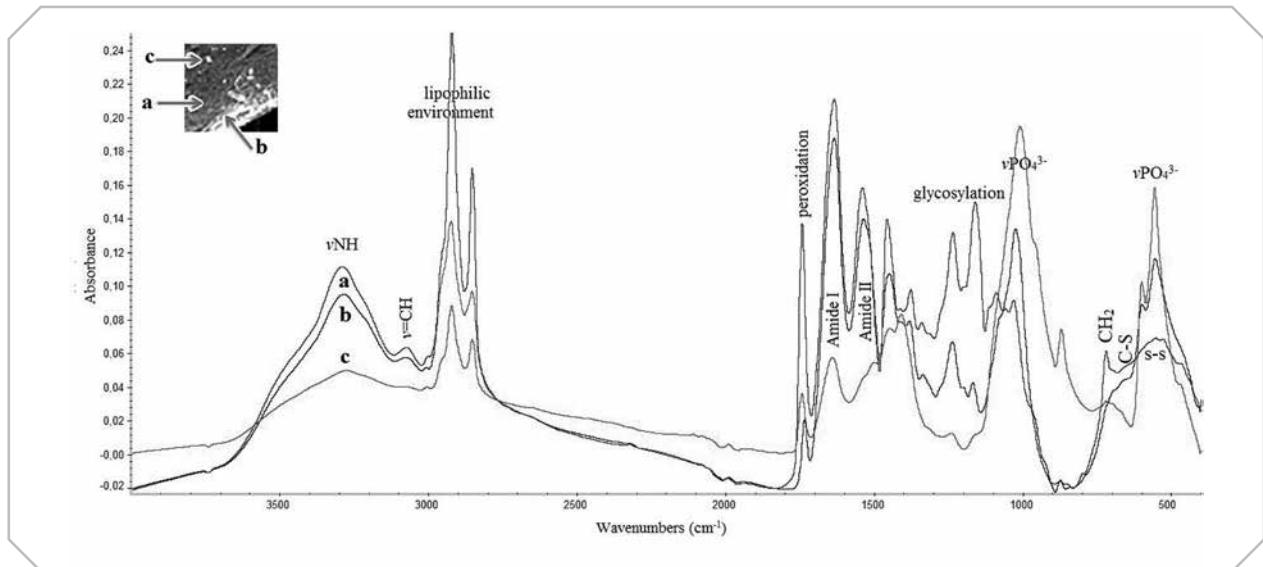


Figure 2. Representative ATR-FT-IR infrared spectra of an aortic valve taken from the spots, **A)** organic phase, **B)** interface between organic and mineral phase and **C)** individual mineral deposit

2.3. X-Ray Diffractometer, XRD

X-ray diffraction analysis was performed using a Siemens D-500 X-Ray diffractometer based on an automatic adjustment and analysis system. The diffraction interval was of 2θ 5° - 70° and scan rate of $0.030^{\circ}/s$.

3. Results

3.1. Infrared spectroscopy

The FT-IR spectra of calcified aortic valve tissue in the region $4,000$ - 400 cm^{-1} are shown in **Figure 2**. The arrows show representative sites of the sample, where the spectra were recorded. Spectrum **a** corresponds to pure organic phase, spectrum **b** was taken at the interface between organic and mineral phase and spectrum **c** is referred to an individual mineral dot, which was at a distance from the main mineralized part of valve tissue.

Comparison between these spectra shows considerable changes in shape and intensity of the bands in all spectral regions, concerning the different components and the conformation from site to site even of the same sample. The characteristic absorption bands and their assignments are given in **Table 2**.

The shoulder band at about $3,495$ cm^{-1} is dominated by absorptions of stretching vibration

of νOH functional groups of hydroxyapatite and structural water molecules. The intensity and the shape of this band is related to the concentration of calcium salts to aortic valve. The intensity of the band at $3,290$ cm^{-1} , which is assigned to stretching vibration of νNH groups of proteins, decreases upon mineralization of the aortic valve, indicating most likely the reduction of the organic phase.

This band is very sensitive and from the slight shift to higher frequencies in interphase region (**Figure 2, spectrum b, Table 2**) it is suggested that the hydrogen bonding interactions of proteins has been changed upon mineralization.

The band at about $3,078$ cm^{-1} is assigned to stretching vibration mode of ($\nu=\text{CH}$) group with olefinic character. This band is used as “marker band” and is related to LDL of the valve.⁸ It was found that the intensity of this “marker band” depended strongly on the lipophilic environment of the tissues and it was independent of the LDL level of the serum and the weight of the patients. On the contrary, the intensity of this band in carotid and coronary arteries was found to be analogous to LDL serum concentration of the patients.^{7,8}

The high intensity bands in the region between $3,000$ - $2,850$ cm^{-1} are assigned to stretching vibration modes of methyl (νCH_3) and methylene (νCH_2)

Table 2. Characteristic band absorption frequencies and their assignments				
Organic a (cm ⁻¹)	Interface b (cm ⁻¹)	Individual c (cm ⁻¹)	Assignment	Reference
3,286	3,295	3,286	ν N-H	7-13
3,183	3,187	3,186	Hb ν N-H	7-18
3,071	3,078	3,077	ν (=C-H ₂), olefinic	7-13
2,960	2,960	2,960	ν_{as} CH ₃	7-17
2,926	2,925	2,924	ν_{as} CH ₂	7-17
2,890			ν CH tertiary	17
2,877	2,877	2,880	ν_{sym} CH ₃	17
2,857	2,857	2,857	ν_{sym} CH ₂	17
-	-	1,746	cholesteric esters	7-9
1,735	1,735		Aldehydes, peroxidation product	7-9
		1,714	Esters ν C=O polar environment	17
1,702	1,700	1,695	Esters ν C=O Hb, β -sheet, antiparallel	7-9
1,685	1,686	1,683	β -sheet, antiparallel	12
1,657	1,658		Amide I α -helix	7-13
1,631	1,631	1,636	Amide I, random coil, β -sheet parallel	7-13
1,597	1,597	1,597	Amide II	7-16
1,541	1,543		Amide II, β -turn, random	7-16
1,511	1,513		β -sheet, parallel	12
1,500	1,499	1,505	C=N	14-17
1,460	1,460	1,454	ν_3 CO ₃ ²⁻ , δ_{as} CH ₂	7-16
1,192	1,192	1,186	ν_{as} HPO ₄ ²⁻ , glycosylation	18,19
1,163	1,165		PO ₂ - of phospholipids	14-16
1,113	1,113	1,115	Glycosylation	12
	1,083	1,077	ν_3 PO ₄ ³⁻	10-12
	1,022	1,024	ν_3 PO ₄ ³⁻	10-12
		1,010	β -Ca ₃ (PO ₄) ₂ , CaHPO ₄	10-12
	956	958	ν_1 PO ₄ ³⁻	10-12
	919	921	HA	10-12
	893	890	HPO ₄ ²⁻	19,20
874	875	874	ν_4 CO ₃ ²⁻	10-12
	724	713	o-o-p-CH ₂ of lipids	14-17
601	601	604	ν_4 PO ₄ ³⁻	10-12
		563	ν_4 PO ₄ ³⁻	10-12
557	557		ν C-S	7-9
521	521		ν S-S	7-9

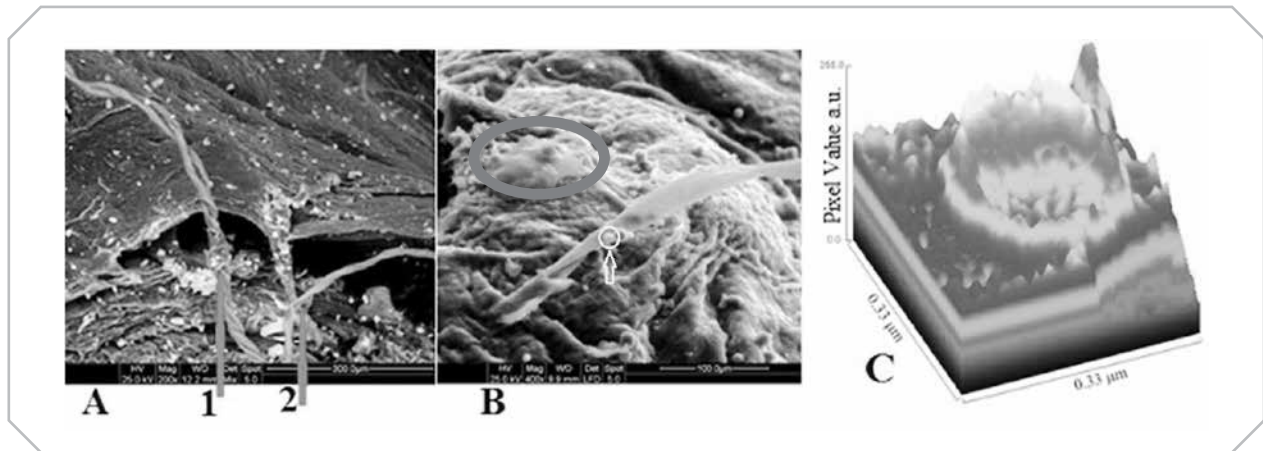


Figure 3. Scanning electron microscope images of morphology and architecture of calcified aortic valve. **A)** general morphology of minerals and fibrils. The arrows 1 and 2 show the fibril and protein branch-polymerization, respectively. (Scale 300 μm , M200x), **B)** Clear view of misfolding proteins and aggregates. The dark grey circle outlines the membrane inflammation. (Scale 100 μm , M400x). **C)** Image J analysis of an aggregate (light white circle in B), showing the barrel configuration

groups. Deconvolution of these bands shows that the bands are not simple, suggesting that the aliphatic chains of lipids interact with high lipophilic environment via aliphatic tails.⁷

3.2. Scanning electron microscope - Energy dispersive X-ray analysis

In order to investigate the surface of the aortic valves we used Scanning electron microscope. The samples were used without any coating of the samples, and thus any change on the architecture of the samples is due only to the disease. **Figure 4** shows the morphology and architecture of the aortic valves. There are shown various pathological alterations and calcification of membranes and collagen fibers that are shown in **Figure 4**. The arrows 1 and 2 in picture A (**Figure 3, A**) show fibril formation and branched proteins polymerization, respectively.

In a higher magnitude of M400x (**Figure 3, B**) the circle outlines the region with a progressive inflammation. Misfolding proteins, fibrils and accumulation of aggregates are found in all valves. The fibrils and aggregates are characteristic of amyloid proteins. ImageJ analysis (**Figure 3, C**) of the white circle and arrow (**Figure 3, B**) confirms the amyloid protein formation since the aggregate have barrel configuration, characteristic scheme

of amyloid proteins. Amyloid is Greek word from amylo, starch, and oid= like and the term was introduced by Rudolf Virchow (1854) to denote a macroscopic tissue abnormality that exhibited a positive iodine staining reaction.

3.3 X-Ray diffraction analysis

XRD analysis (**Figure 4**) demonstrates that calcium deposits in the aortic valve tissues are consistent with biological hydroxyapatite, $(\text{Ca}_{10}(\text{PO}_4)_6(\text{OH})_2)$, as in bones, and different calcium phosphate salts, such as dicalcium phosphate, CaHPO_4 , tricalcium phosphate, $\text{Ca}_3(\text{PO}_4)_2$, formed from phospholipid fragments.

The XRD results are in accordance with infrared data, which also were denoted by infrared spectra. The amorphous salts cannot be detected by XRD.

4. Discussion

The FT-IR spectra of aortic valves, in combination with SEM-EDX and XRD analysis show important changes which are related with the progression of the disease. The appearance in the aortic valves' infrared spectra of the band at $3,075\text{ cm}^{-1}$, which is a "marker band" for oxidized LDL, leads to the suggestion that peroxidation of lipids takes place in the pathways of aortic valve calcification. This band depends on LDL of the aortic valves and not on the serum LDL concentration of the patients. This

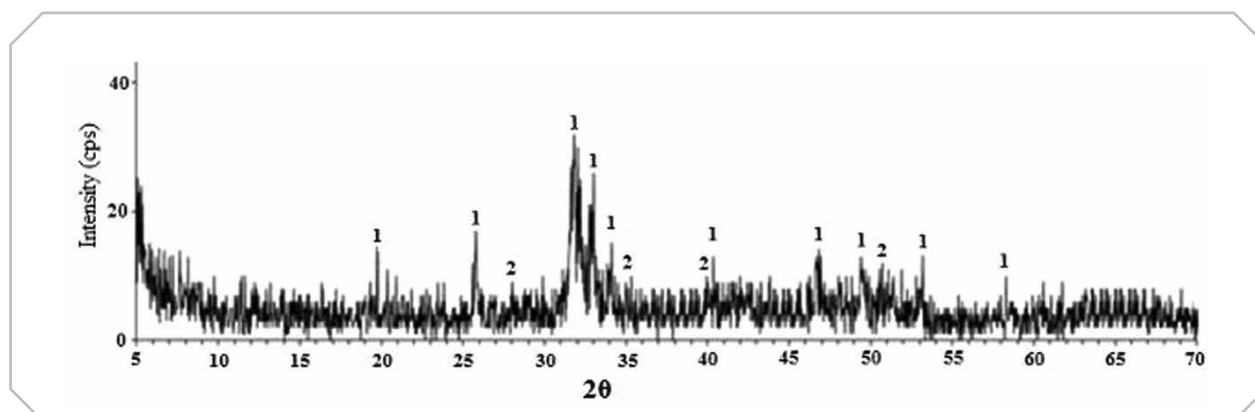


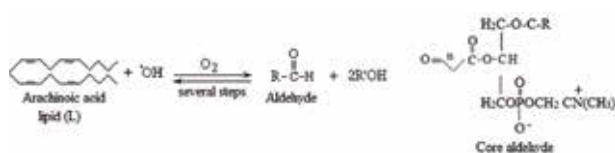
Figure 4. XRD diagram of calcified aortic valve. 1: biological hydroxyapatite, $\text{Ca}_{10}(\text{PO}_4)_6(\text{OH})_2$, and 2: dicalcium phosphate, $\text{Ca}_2\text{HPO}_4\text{W}$

band is used as “marker band” for the progression of sclerosis. These findings are in accordance with observations of Novaro and Griffin who found that serum lipoprotein levels closely correlate with the presence of aortic sclerosis but they are independent on LDL levels.²¹ The above fact leads to the suggestion that oxidative stress activates inflammation mechanisms followed by the progression of atherosclerotic lesions.

This hypothesis is supported from the presence of the high density absorption band at $1,744\text{ cm}^{-1}$, which corresponds to carbonyl stretching vibration of phospholipid esters, cholesteric esters and aldehydes. It is observed that the intensity of this band increases in the organic region and in the interface and it is decreased in single mineral phase of the sample (**Figure 2, C**). These data illustrate the strongly dependence of the formation of oxidation products of lipid and phospholipid, such as LDL cholesterol. The appearance in the spectra of an absorption band at $1,734\text{ cm}^{-1}$ indicates the presence of aldehydes in aortic valve tissues due to lipid peroxidation and especially of arachidonic acid.²² Salaris and Babbs using the Wistar rats model found strong dependence of malondialdehyde-like materials formation and ischemia/reoxygenation process,²³ which is in agreement with our results.

The production of aldehydes is related to membrane cell damage. In order to explain the production of aldehydes we accepted that the hydroxyl free radicals which are produced during

metabolism or oxidative stress interact with lipids producing lipid peroxides (LOO). These peroxides are not stable and decompose, generating free radicals, core aldehydes and ketones that covalently modify ϵ -amino groups of lysine residues of the protein moiety⁷ as follows:



This mechanism is believed to take place in the organism during the first face of oxidation of arachidonic acid from prostaglandine H synthetase.²⁴

Deconvolution of the band at $1,734\text{ cm}^{-1}$ (not shown here) suggests that the ester $\nu\text{C}=\text{O}$ group interacts in different ways with lipophilic environment. In the case of the individual mineral, (**Figure 2, spectrum C**) the band at 1714 cm^{-1} indicates that the ester $\nu\text{C}=\text{O}$ group is located in polar environment. This band does not appear in the spectra of organic environment or in interface. Furthermore, these data indicate that regions rich in oxidized lipids are preferential sites for mineral deposition.

The absorption bands in the spectral region $1,700\text{ cm}^{-1}$ to $1,500\text{ cm}^{-1}$ are similar to those generated by a combination of the $\nu\text{C}=\text{O}$ stretching and the δNH bending vibrations of the amide I and amide II modes of protein peptide bond ($-\text{NHCO}-$).¹³⁻¹⁶ The bands at $1,629$ and $1,543\text{ cm}^{-1}$ are attributed to

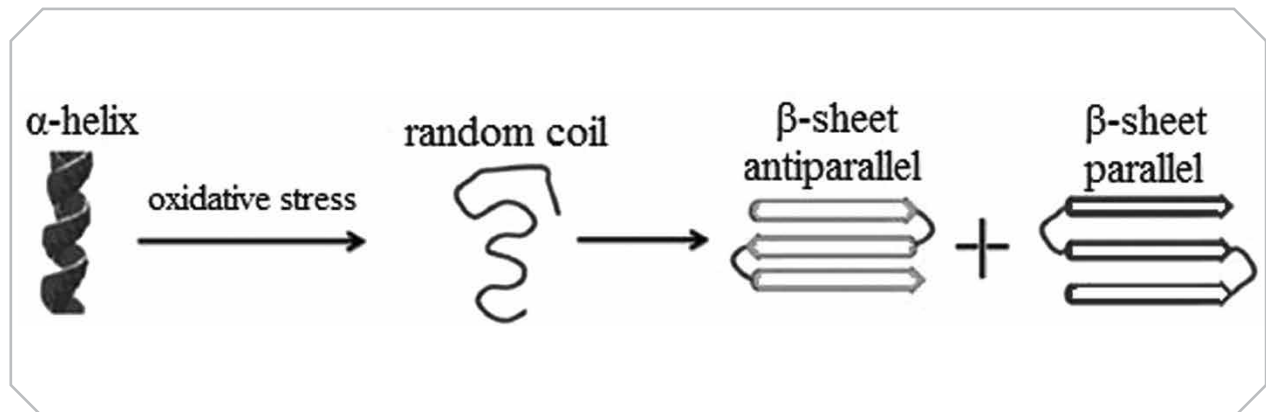


Figure 5. Schematic presentation of protein conformational changes from α -helix to random coil and amyloid formation (β -sheet // and anti-//)

amide I and amide II vibrations, respectively. These bands are shifted to lower frequencies, comparing with the absorption of healthy tissues, which are found at 1,655 and 1,555 cm^{-1} . These shifts are associated with the change of proteins and collagen secondary molecular structure from α -helix to random coil and β -turns.^{8,13-17} Furthermore, intensity and shift changes of the bands in the region 1,600-1,510 cm^{-1} , are correlated with the decrease of the ApoI/ApoII, which corresponds to HDL and controls the LDL.⁸ The bands in the region 1,700-1,680 cm^{-1} (β -antiparallel sheet) and that about 1,513 cm^{-1} (β -parallel sheet) indicated the formation of amyloid-like proteins (**Figure 5**).

Amyloid proteins are characterized from their non-specific sequence and their folding configuration, which is known as cross β -structure and form aggregates.¹² Furthermore, ImageJ analysis of aggregates (**Figure 3, C**) confirms the formation of amyloid proteins and their barrel conformation. The formation of amyloid proteins is also supported by the high intensity bands in the region 3,000-2,800 cm^{-1} , where the stretching vibration of methyl and methylene groups of lipids appear. The disappearance of the asymmetric stretching vibration of methyl group ($\nu_{\text{as}}\text{CH}_3$) is an evidence of the high order of the membrane lipids, due to high lipophilic environment, as a result of amyloid protein formation. The oxidative stress induced amyloid protein production and this must be taking it in consideration in the early stages of the disease.

The spectral region between 1,200-850 cm^{-1} exhibit the characteristic asymmetric and symmetric stretching modes of PO_2 of DNA, phosphodiester groups of the phospholipids, cholesterol ester and $-\text{C}-\text{O}-\text{C}-$ vibrations of fatty acids and ketals.¹⁸⁻²⁰

As it is shown, in spectrum **a** (**Figure 3, A**) there are significant changes in shape and intensity of the bands, resulting from the organic face. On the contrary, at the other two spectra the main bands correspond to characteristic vibrations of the phosphate groups of hydroxyapatite. The band at about 1,190-1,192 cm^{-1} is attributed to asymmetric stretching vibration of $\nu_{\text{as}}\text{HPO}_4^{2-}$, suggesting that the initiation of mineral formation requires a polar environment. This result is confirmed with XRD analysis due to the presence of Ca_2HPO_4 (**Figure 3**). In the case of the individual mineral dot (**Figure 2, C**) appears a high intensity band at 1,010 cm^{-1} , which is attributed to phosphate groups of calcium phosphates. This indicates the presence of $\beta\text{-Ca}_3(\text{PO}_4)_2$ components.²⁵ Deconvolution of this band shows that it is not a simple band suggesting that there is not only bone formation as hydroxyapatite, but there are also other calcium salts, resulting most likely from phospholipid fragmentation due most likely to carbon chain fragmentation of the phospholipids.⁷

The presence of Ca_2HPO_4 salts leads to the suggestion that during the salt formation an acid pH environment was formed in the patient and that acidosis and anaerobic conditions induce oxidative

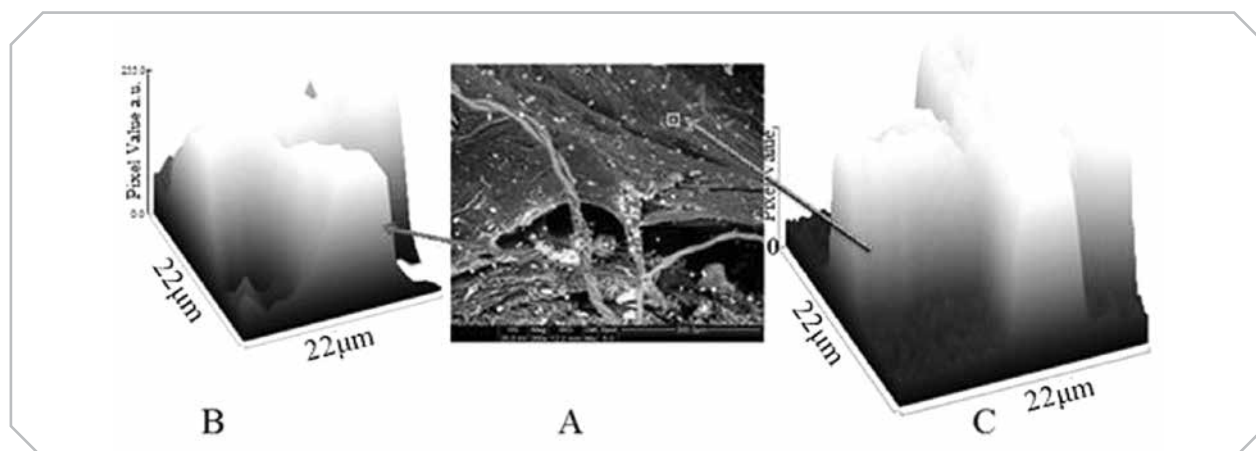


Figure 6. A) Scanning electron microscope morphology of calcified aortic valve. B) ImageJ analysis of branched proteins and C) Image J analysis of cross-linked proteins

hydrolysis of Adenosine Triphosphate (ATP) affecting calcium homeostasis. It was proposed first by Drury and Szent-Györgyi²⁶ that ATP is required for myocardial contracture and relaxation, as well as maintenance of normal myocardial impulse conduction. It was observed that depletion of ATP increases 3-fold the production of Pi (inorganic monophosphates, PO_4^{3-}) at the end of ischemic perfusion.²⁷ Recent research data also indicate that ATP phosphorylation regulation plays an important role in aortic valve calcification.²⁸ The presence of calcium carbonate anions in the infrared spectra (**Table 2**) demonstrates that carbon dioxide accumulation takes place, which results in carbonic acid (H_2CO_3) sustaining further the acidity of the environment.

SEM-EDEX analysis shows that the molar ratio of Ca/P varies and that magnesium, a calcium antagonist, substitutes the calcium ions producing more soluble phosphate salts. This substitution inhibits the bone formation and maybe aortic valve stenosis⁹. Our results show that in order to reduce the progression of calcification of aortic valves a treatment of patients with magnesium salts must be applied. Magnesium cations (Mg^{2+}) are known to regulate ATP metabolism and are cofactor in more than 300 intracellular enzymes.²⁹ It is known that Mg^{2+} inhibits the release of Ca^{2+} from the sarcoplasmic reticulum, blocking the influx of Ca^{2+} into the cell by inactivating the Ca^{2+} channels

in the cell membrane, and competes with Ca^{2+} at binding sites on troponin C and myosin, thereby inhibiting the ability of Ca^{2+} cations to stimulate myocardial tension.³⁰ Additionally, ImageJ analysis of mineralized regions confirms that in the early stages, calcium phosphate salts are deposited and organized structurally into the specific pattern of the cross-linked and branched bonds of proteins (**Figure 6**).

These findings strongly support the hypothesis that during the progression of the valve sclerosis and mineralization protein free radicals are produced, which give stable final products linear-, branched- or cross-linked co-polymers and that these reaction take place at the sites of sulfur (S) atoms of proteins, producing a disulfide S-S bond. The sites of the cross-linked and branched chemical bonds seem to be the target of development and progression of the mineral deposition.

The production of disulfide bonds is shown from the absorption bands in the region 600-400 cm^{-1} , where are located the characteristic absorption bands of the groups S-S and C-S (**Figure 2, A and Table 2**). In addition, glutathione (gamma-glutamyl-cysteinyl-glycine; GSH) is the most active endogenous antioxidant, which interacts with free radicals inhibited the damage of lipids and thus protects the cardiovascular system. Furthermore, glutathione is known to react as donor of hydrogen atoms repairing in this way the damaged lipids.

In both cases are produced S-S bonds, leading to a deficiency of endogenous antioxidants.^{7,9}

5. Conclusions

The research study demonstrates that FT-IR spectroscopy is a powerful tool to investigate the aortic valve calcification and amyloid-like protein formation. The characteristic ATR-FT-IR absorption bands and their changes of aortic valve are linked with hyperoxidation of membranes due to free radical formation during a pro-inflammation stage and amyloid protein formation. The shifts of the absorption bands Amide I and Amide II groups in the spectral region 1,700-1,500 cm^{-1} are strongly correlated with amyloid-like protein formation and progression of the disease. From the shape and the frequencies of the bands in the region 1,200-950 cm^{-1} it is indicated that the mineral deposits

are low crystallinity biological hydroxyapatite ($\text{Ca}_{10}(\text{PO}_4)_6(\text{OH})_2$). SEM-EDAX and XRD data show that substitution of Ca^{2+} cations by Mg^{2+} cations leads to amorphous hydroxyapatite formation. This substitution we believe that it prevents aortic valve stenosis. It also suggests that treatment with magnesium salts maybe could avoid the calcification of aortic valves.

Moreover, our findings strongly support the hypothesis that oxidative stress is involved during the progression of the valve mineralization amyloid protein formation, giving stable final products linear-, branched- or cross-linked co-polymers. The most sensitive sites are the sulfur (S) atoms of proteins and S-S bonds. \square

Conflict of interest: All authors declare no conflict of interest.

Περίληψη

Σχηματισμός αμυλοειδούς τύπου πρωτεϊνών και επασβέστωση της αορτικής βαλβίδας λόγω οξειδωτικού στρες

I. Μαμαρέλης¹, E. Κουτουλάκης², X. Κωτούλας³, B. Δρίτσα³, B. Μαμαρέλη³, K. Πισσαριδη⁴, M. Κυριακίδου³, I. Αναστασοπούλου^{4,5}

¹Καρδιολογική Κλινική ΝΙΜΤΣ

²Καρδιολογική & ³Καρδιοχειρουργική κλινική 401 Γενικό Στρατιωτικό Νοσοκομείο Αθηνών

⁴Ακτινοχημεία & Βιοφασματοσκοπία, Σχολή Χημικών Μηχανικών, Εθνικό Μετσόβιο Πολυτεχνείο Πολυτεχνειούπολη Ζωγράφου, 15780 Αθήνα,

⁵Διεθνές Αντικαρκινικό Ερευνητικό Ινστιτούτο, 1ο χιλ. Καπανδριτίου - Καλάμου, Καπανδρίτι, Αττική, 19014

Ημελέτη του μηχανισμού επασβέστωσης και στένωσης της αορτικής βαλβίδας κατά τη διάρκεια του οξειδωτικού στρες έγινε με υπέρυθρη φασματοσκοπία με μετασχηματισμό Fourier αποσβένουσας ολικής ανάκλασης, ηλεκτρονικό μικροσκόπιο σάρωσης και διαθλασίμετρο ακτίνων Χ. Η υψηλής έντασης ταινίες των δονήσεων τάσης των ομάδων νCH₃ και νCH₂ των λιπιδίων των μεμβρανών συνδέονται με την αύξηση του λιπόφιλου περιβάλλοντος, λόγω του σχηματισμού αμυλοειδούς-τύπου πρωτεϊνών. Οι μετατοπίσεις προς χαμηλότερες συχνότητες των απορροφήσεων των Amide I και Amide II δείχνουν την μεταβολή της διαμόρφωσης των πρωτεϊνών από α-έλικα σε β-παράλληλα και β-αντιπαράλληλα επίπεδα, ως αποτέλεσμα του σχηματισμού αμυλοειδών πρωτεϊνών. Ο σχηματισμός υδροξυαπατίτη (Ca₁₀(PO₄)₆(OH)₂) και CaHPO₄ διαπιστώθηκαν από την ανάλυση με διαθλασίμετρο ακτίνων Χ. Τα δεδομένα έδειξαν ότι το οξειδωτικό στρες είναι ένα από τα μονοπάτια σχηματισμού αμυλοειδούς τύπου πρωτεϊνών, το οποίο οδηγεί στην επασβέστωση της αορτικής βαλβίδας, κυρίως σε θέσεις των δισουλφικών δεσμών (S-S).

Λέξεις ευρητηρίου: επασβέστωση αορτικής βαλβίδας, στένωση αορτικής βαλβίδας, αμυλοειδείς πρωτεΐνες, υπέρυθρη φασματοσκοπία με μετασχηματισμό fourier, ηλεκτρονικό μικροσκόπιο σάρωσης, διαθλασίμετρο ακτίνων Χ

***Στοιχεία υπεύθυνου συγγραφέα:** Ιωάννα Αναστασοπούλου

Εθνικό Μετσόβιο Πολυτεχνείο, Σχολή Χημικών Μηχανικών, Ακτινοχημεία & Βιοφασματοσκοπία, Πολυτεχνειούπολη Ζωγράφου, 15780 Ζωγράφου. Τηλ. Επικοινωνίας: 6973013308, E-mail: ianastas@central.ntua.gr

References

1. Lindroos M, Kupari M, Heikkilä J, et al. Prevalence of aortic valve abnormalities in the elderly: An echocardiographic study of a random population sample. *J Am Coll Cardiol* 1993, 21:1220–1225
2. Stewart BF, Siscovick D, Lind BK, et al. Clinical factors associated with calcific aortic valve disease. Cardiovascular Health Study. *J Am Coll Cardiol* 1997, 29:630–634
3. Pflederer T, Achenbach S. Aortic valve stenosis: CT contributions to diagnosis and therapy. *J Cardiovasc Comput Tomogr* 2010, 4:355–364
4. Otto CM, Lind BK, Kitzman DW, et al. Association of aortic-valve sclerosis with cardiovascular mortality and morbidity in the elderly. *N Engl J Med*. 1999, 341:142–147
5. Roosens B, Bala G, Droogmans S, et al. Animal models of organic heart valve disease. *International Journal of Cardiology* 2013, 165: 398–409
6. Rajamannan NM. Calcific Aortic Stenosis: Lessons Learned from Experimental and Clinical Studies. *Arterioscler Thromb Vasc Biol*. 2009, 29:162–168
7. Mamarelis I., Pissaridi K, Dritsa V, et al. Oxidative Stress and Atherogenesis an FT-IR Spectroscopic Study. *In Vivo* 2010, 24: 883–888
8. Mamarelis I, Pissaridi K, Dritsa V, et al. The effect of molybdenoenzymes on atherosclerotic hyperuricemic patients. In Basil S. Lewis, Moshe Y. et al. (eds), Coronary Artery Disease. *International Proceedings* 2011, 83–90
9. Dritsa V, Pissaridi K, Koutoulakis E, et al. An Infrared Spectroscopic Study of Aortic Valve. A Possible Mechanism of Calcification and the Role of Magnesium Salts. *In Vivo* 2014, 28: 91–98
10. Petra M, Anastassopoulou J, Theologis T, et al. Synchrotron micro-FT-IR spectroscopic evaluation of normal paediatric human bone. *J. Mol Structure* 2005, 78: 101–116
11. Anastassopoulou J, Kolovou P, Papagelopoulos P, et al. The role of β -antagonists on the structure of human bone A spectroscopic study. In: T. Theophanides (ed). *Infrared Spectroscopy–Life and Biomedical Science*. *Intech Publications* 2012, 271–288
12. Anastassopoulou J, Kyriakidou M, Kyriazis S, et al. Protein folding and cancer. *Anticancer Res* 2014, 34: 5806–5709
13. Anastassopoulou J, Boukaki E, Conti C, et al. Micro-imaging FT-IR spectroscopy on pathological breast tissues. *Vibrational Spectroscopy* 2009, 51:270–275
14. Theophanides T. Infrared Spectroscopy-Anharmonicity of Biomolecules, Crosslinking of Biopolymers, Food Quality and Medical Applications. *InTech Publications* 2015
15. Theophanides T. Infrared Spectroscopy. Life and Biomaterial Sciences. Croatia. Rijeka, *Intech Publications* 2015
16. Theophanides T. Infrared Spectroscopy: Anharmonicity of Biological Molecules, Crosslinking of Biopolymers, Food Quality and Medical Applications. Book 3. Rijeka, *Intech Publications* 2015
17. Bellamy JL. The infrared spectroscopy of complex molecules, 3rd Edition, *Chapman and Hall* 1975
18. Dritsa V. FT-IR spectroscopy in medicine. In Theophanides T (ed). *Infrared Spectroscopy. Life and Biomaterial Sciences*. *Intech Publications* 2012, 271–288
19. Holt C, Van Kemenade MJJM, Harries JE, et al. Preparation of amorphous calcium-magnesium phosphates at pH 7 and characterization by X-ray absorption and Fourier transform infrared spectroscopy. *J Cryst Growth* 1988, 92:239–252
20. Holt C, Van Kemenade MJJM, Nelson Jr, et al. Amorphous calcium phosphates prepared at pH 6.5 and 6.0. *Mat. Res. Bull* 1989, 23:55–62
21. Novaro GM, Griffin BP. Calcific aortic stenosis: Another face of atherosclerosis? Heart Valve Update. *Cleveland Clinic J Medicine* 2003, 70:471–477
22. Kristal BS, Park BK, Yu BP. 4- hydroxyhexenal is a potent inducer of the mitochondrial permeability transition. *J. Biol. Chem* 1996, 271:6033–6038
23. Salaris S C. Babbs CF. Effect of oxygen concentration on the formation of malondialdehyde-like material in a model of tissue ischemia and reoxygenation. *Free Radical Biol Med* 1989;7: 603–609
24. Smith WL, Garavito RM, DeWitt DL. *J Biol Chem* 1996, 271:33157–33160

25. Fowler BO, Moreno E C, Brown W E. Infra-red spectra of hydroxyapatite, octacalcium phosphate and pyrolysed octacalcium phosphate, *Arch oval Biol.* 1966, 11: 477-492
26. Drury N, Szent-Gyorgyi A. The physiological activity of adenine compounds with special reference to their action upon the mammalian heart. *J Physiol* 1929, 68: 213-237
27. Cave AC, Ingwall JS, Friedrich J, et al. ATP Synthesis During Low-Flow Ischemia, Influence of Increased Glycolytic Substrate. *Circulation* 2000, 101:2090-2096
28. Cote N, El Husseini D, Pépin A, et al. ATP acts as a survival signal and prevents the mineralization of aortic valve. *J Mol Cellular Cardiology* 2012, 52: 1191-1202
29. Theophanides T, Anastassopoulou J. Magnesium: Current status and new developments. *Kluwer Academic Publishers* 1997
30. Iseri LT, French JH. Magnesium: Nature's physiological calcium blocker. *Am Heart J* 1984, 108:188-194